

# Evaluation of Corrosion Property of Aluminium-Zirconium Dioxide (AlZrO<sub>2</sub>) Nanocomposites

M. Ramachandra, G. Dilip Maruthi, R. Rashmi

**Abstract**—This paper aims to study the corrosion property of aluminum matrix nanocomposite of an aluminum alloy (Al-6061) reinforced with zirconium dioxide (ZrO<sub>2</sub>) particles. The zirconium dioxide particles are synthesized by solution combustion method. The nanocomposite materials are prepared by mechanical stir casting method, varying the percentage of n-ZrO<sub>2</sub> (2.5%, 5% and 7.5% by weight). The corrosion behavior of base metal (Al-6061) and Al/ZrO<sub>2</sub> nanocomposite in seawater (3.5% NaCl solution) is measured using the potential control method. The corrosion rate is evaluated by Tafel extrapolation technique. The corrosion potential increases with the increase in wt.% of n-ZrO<sub>2</sub> in the nanocomposite which means the decrease in corrosion rate. It is found that on addition of n-ZrO<sub>2</sub> particles to the aluminum matrix, the corrosion rate has decreased compared to the base metal.

**Keywords**—Al6061 alloy, corrosion, solution combustion, stir casting, Potentiostat, Zirconium Dioxide.

## I. INTRODUCTION

METAL matrix composites (MMCs) are significant class of materials. With non-metallic reinforcements incorporated in metal matrices, enhancement in material properties can be witnessed. When compared to monolithic and conventional alloys of the metal, MMCs will attain high strength and stiffness [1]. In view of this, Al 6061 as matrix material and reinforcing it with zirconium particles result in MMCs with high specific strength for various light weight applications [2]. Aerospace and automobile industry uses widely Al-based MMCs for its various components and also Al-based MMCs are used in architectural applications. Over the last three decades, particles reinforced MMCs have been the most popular and among the MMCs, ceramic reinforced Al-MMCs are finding wide applications. Incorporation of the second phase particulate into an aluminum matrix material will enhance the mechanical properties of the base aluminum metal; it will significantly change the corrosion properties and its behavior [3]. Particulate reinforced MMCs can result in an increase in strength and stiffness at much lower additional costs than those of continuous reinforcements like fibers [4].

Metal matrix nanocomposites (MMNCs) with the addition of nano-sized ceramic particles can be of significance for automobile, aerospace, and numerous other applications. The physical and mechanical characteristics of the light refractory carbides such as SiC, TiC, and B<sub>4</sub>C make them suitable for

being used as reinforcement in aluminum based MMCs. An attempt has been made to investigate the inexpensive fabrication of bulk lightweight MMNCs with reproducible microstructures and superior properties by use of ultrasonic nonlinear effects, namely transient cavitation and acoustic streaming to achieve uniform dispersion of nano-sized B<sub>4</sub>C particles in molten aluminum alloy and found that mechanical properties of the cast MMNCs have been improved significantly even with a low weight fraction of nano-sized B<sub>4</sub>C [5].

Zirconia and zirconia stabilized by yttria, YSZ-reinforced Ni-composite coatings were developed by electro deposition method. It was observed from the micro hardness studies that there is no significant difference in the values for Ni-SiC and Ni-ZrO<sub>2</sub> coatings. Using polarization and electrochemical impedance studies corrosion properties were evaluated. The studies showed that oxide particle-reinforced Ni coatings possessed better corrosion resistance due to their lower corrosion current density. Wear and corrosion studies were carried out to understand the synergistic effect of wear and corrosion on the performance of Ni-based composite coatings in 0.5 M Na<sub>2</sub>SO<sub>4</sub>. Among various composite coatings, Ni-YSZ exhibited less material loss thereby showing better tribo-corrosion behavior [6].

Nanostructures materials (1–100 nm) are known for their outstanding mechanical and physical properties due to their extremely fine grain size and high grain boundary volume fraction [7]. Significant progress has been made in various aspects of synthesis of nano-scale materials. The focus is now shifting from synthesis to manufacture of useful structures and coatings having greater wear and Corrosion resistance.

Zn-carbon nanotubes composite coatings were obtained from a sulphate bath containing dispersed carbon nanotubes (CNTs). The electrochemical and weight loss measurements were made to find the corrosion behavior of composite coating. The presence of carbon nanotubes shifts the potential of zinc deposit to more positive values. The composite coatings were porous free and the service life of coating was examined by salt spray test. The electrochemical studies revealed higher resistance of composite coatings to corrosion. The surface morphology was investigated by recording the SEM images of coating before and after corrosion. The mechanism of action against corrosion was established [8]

Natural process of corrosion transforms unstable refined metals to their more stable oxide state. Corrosion is gradual destruction of metals by chemical reaction with the gases present in the environment. Electrochemical oxidation of metal where there is a reaction with an oxidant such as oxygen

M. Ramachandra, Professor in Mechanical Engineering, is with the BMS College of Engineering, Bengaluru, Karnataka- India (phone: +91 9448819945; e-mail: ramachandram.mech@bmsce.ac.in).

G. Dilip Maruthi and R. Rashmi are Assistant Professor in Mechanical Engineering, BMS College of Engineering, Bengaluru, Karnataka, India (e-mail: gdm.mech@bmsce.ac.in, rashmir.mech@bmsce.ac.in).

in the air is called as corrosion. Popularly known as rusting is the formation of iron oxides is a well-known example of electrochemical corrosion. Corrosion is considered as a type of damage that typically produces oxides or salts of the original metal. Materials like ceramics and polymers also undergo corrosion reaction. Corrosion degrades the useful properties of base materials and structures including strength, appearance, and permeability to liquids and gases.

## II. SYNTHESIS OF ZIRCONIA AND NANOCOMPOSITES

### A. Materials

Al-6061 is a light weight metal which is selected as matrix material due to its many advantageous properties. Al-6061 exhibit many essential properties that can be useful in manufacturing and production field. It exhibits excellent casting properties, strength, formability, and heat treatable [9]. Amorphous zirconium dioxide ( $ZrO_2$ ) with average size of 50 nm is used as reinforcement material in Al-6061 matrix material. It has density of 5.68 gm/cc.  $ZrO_2$  at room temperature is considered to be an important structural ceramic because of its excellent mechanical properties, such as fracture toughness, high strength, and hardness. It is also an important material because of its use in different fields of chemistry such as ceramics and as catalyst. Ceramics made with  $ZrO_2$  are known to show a good improvement in strength and toughness.

### B. Synthesis of n- $ZrO_2$

Nano- $ZrO_2$  particulates are synthesized by solution combustion method. A through mixture of 5 g of zirconyl nitrate along with the calculated amount of the fuel urea and 25 ml of distilled water is prepared in a Petri dish (having dimensions 100 mm x 50 mm). For thorough mixing, a magnetic stirrer is used for about 15 min and at the end of mixing a homogenous solution is obtained. A pre heated muffle furnace for about 500 °C for firing the fuel urea. The crystalline dish containing the homogenous solution is placed in the muffle furnace for boiling which yields a viscous liquid which then spontaneously catches fire due to the high exothermic process and homogeneous solution gets converted in to a flaky type powder. Fig. 1 (a) shows firing of aqueous solution. The dish is left in the furnace for furnace cooling and until all the fumes of carbon dioxide, nitrogen and steam emanating from is subsided. The dish containing the flaky powder of  $ZrO_2$  is then taken out and allowed to cool further in open atmosphere. The contents of the dish containing the flaky powder of  $ZrO_2$  are transferred to a grinder and are ground into a fine powder to get nano-sized  $ZrO_2$ . Fig. 1 (b) shows synthesized n- $ZrO_2$  powder. The above process yields only 1.5 g of n- $ZrO_2$  powder for the said quantities of the homogeneous mixture. Thus, the solution combustion process is repeated a number of times to get an adequate amount of n- $ZrO_2$  required for casting and studies.

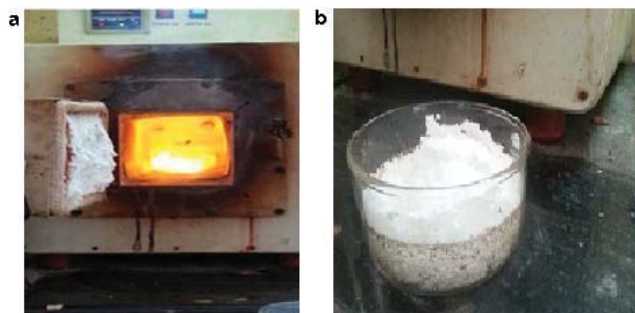


Fig. 1 Combustion synthesis method is used to synthesize n- $ZrO_2$

### C. Synthesis of Nanocomposites

The nanocomposite of Al-6061/ $ZrO_2$  is prepared by mechanical stirrer using vortex technique. The various manufacturing techniques are stir casting [9]-[14], squeeze casting [16], exothermic dispersion [15] and infiltration method [17], [18]. The cleaned base metal Al-6061 ingots are melted to the desired super heating temperature of 800 °C in graphite crucibles under a cover of flux using 3-phase electrical resistance furnace. The molten metal is degassed at a temperature of 780 °C. Amorphous zirconium dioxide particulates, preheated to around 650 °C are then added to the molten metal and stirred continuously. Stirring time is maintained between 5–8 minutes at an impeller speed of 600 rpm. During stirring, magnesium is added in small quantities to increase the wettability of particles. The dispersion of the preheated Zirconium dioxide particulates is achieved in accordance with the vortex method. The melt with the reinforced particulates are poured into the dried, coated, cylindrical permanent metallic molds of size 50mm diameter and 175 mm height. The pouring temperature is maintained at 700 °C. The melt is allowed to solidify in the molds. For the purpose of comparison, the base alloy is cast under similar processing conditions as described. The nMMC processing arrangement is shown in Fig. 2. The proportion of  $ZrO_2$  is varied from 0 wt.% to 7.5 wt.% in steps of 2.5 wt.%.

TABLE I  
CHEMICAL COMPOSITION OF NANOCOMPOSITES

S. N	Percentage of Aluminum (% by wt.)	Percentage of Zirconium Dioxide (% by wt.)
1	100	0
2	97.5	2.5
3	95	5
4	92.5	7.5

### D. Specimen Preparation

The cylindrical blocks of Al-6061 base metal reinforced with  $ZrO_2$  produced after casting are machined into the rectangular specimens of length 20 mm, breadth 10 mm, and thickness 10 mm for standard test. The specimens are sealed with epoxy resin leaving a flat surface of area 50 mm<sup>2</sup>. The exposed flat surface is polished with emery papers to 600 grit level and cleaned with acetone and dried.

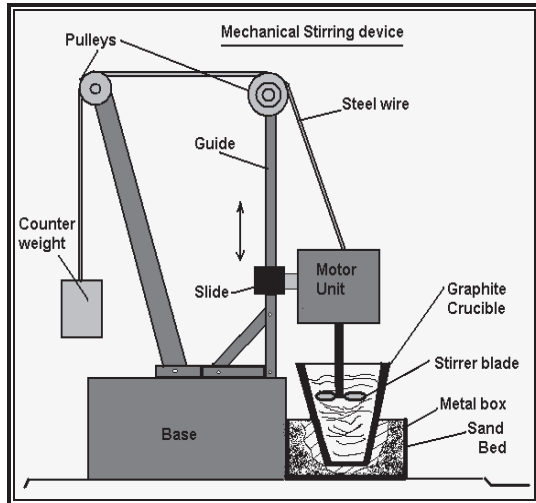


Fig. 2 n-MMC processing arrangement

### E. Corrosion Test

All metals whether it is pure or an alloys are susceptible to corrosion. It is the degradation of metal by converting metal into their stable oxides. All corrosion is an electrochemical process of oxidation and reduction. As corrosion occurs, electrons are released by metal (oxidation) and gained by elements (reduction) in the corroding solution [5]. Controlled electrochemical experimental method is used to characterize the corrosion properties [5]-[8]. For this experiment, the set up consist of three electrodes which are connected to the electronic CH instrument called Potentiostat (Fig. 3). The electrodes used are:

1. Specimen – Working electrode
2. Saturated Calomel electrode – Reference electrode
3. Platinum – Counter electrode



Fig. 3 CH instrument used for measuring the rate of corrosion

All three electrodes are placed in the electrolyte solution of 3.5% NaCl solution (approximate sea water). The rectangular specimens of length 20 mm, breadth 10 mm, and thickness 10 mm are prepared by adopting standard metallographic procedure [6]. The specimen is used as a working electrode and corrosion test is conducted further. Fig.1 shows the arrangement of electrochemical testing which is used for corrosion test. The finely polished Al-6061/ZrO<sub>2</sub> Nanocomposite specimens are exposed to corrosion medium

with its exposing surface area 1 mm<sup>2</sup>. The potentiodynamic current potential curves are recorded by polarizing the specimen to -1.5 V cathodically and -0.9 V anodically using open circuit potential (OCP) at a scan rate of 0.01 V/s. In this experiment, Tafel equation is used to calculate the corrosion rate from the achieved polarization result.

## III. RESULTS AND DISCUSSION

### A. Synthesis of n-ZrO<sub>2</sub>

For phase identification the synthesized, n-ZrO<sub>2</sub> powder is analyzed by using X-ray diffraction analyzer (XRD). Finely ground ZrO<sub>2</sub> is homogenized and average bulk composition is determined. XRD analysis procedure involves preparation of specimen, mounting of the specimen in the slide and XRD apparatus activation. In the diffractogram, the intensity of the diffraction signal is plotted against the diffraction angle 2θ degrees.

The XRD pattern obtained for n-ZrO<sub>2</sub> closely conforms to the standard XRD pattern as shown in Fig. 4 where the significant peaks of the standard XRD pattern occur at around the following diffraction angles 2θ=30°, 2θ=35°, 2θ=50°, and 2θ=60°. There are some tiny peaks which occur at certain angles corresponding to the impurities present in the sample powder and hence represent very less impurities. Peak positions and approximate relative intensities in Fig. 4 represent the phases present in the sample. Nano-ZrO<sub>2</sub> prepared using urea as fuel at 500 °C exhibited only a single cubic and mono clinic phase. The size of the synthesized n-ZrO<sub>2</sub> is in the Nano scale as seen in scanning electron micrograph (Fig. 5), aluminum and ZrO<sub>2</sub> phases present are identified clearly, and negligible impurities are found in the sample.

### B. Microstructure

Scanning Electron Micrograph (SEM) of ZrO<sub>2</sub> is shown in Fig. 5. The average particulate size is found to be 50 nm. In Fig. 6 the distribution of ZrO<sub>2</sub> is found to be near uniform and Fig. 7 shows good interfacial bonding between ZrO<sub>2</sub> and Aluminium matrix. It is clear that the nano particulates were successfully embedded in the Al matrix. According to the aforementioned results, it can be concluded that the production of bulk nanocomposites using conventional stir casting is effective. The ZrO<sub>2</sub> nanoparticles distribution in the Al matrix was fairly uniform, although small agglomerates in ZrO<sub>2</sub> nanocomposites still existed in the matrix.

### C. Corrosion Test

Figs. 8-11 show the rate of corrosion for different composition of ZrO<sub>2</sub> in the nanocomposite. The graphs of current vs potential are plotted which show the rate of corrosion in the different composition. In Fig. 8, the graph shows the potential of 1.29 mV, which gradually increases with increase in percentage of ZrO<sub>2</sub>. Table II shows the different corrosion potential obtained for different chemical composition. The potentiodynamic polarization curves for the composites in NaCl solution helped in analysing more thoroughly the corrosion behaviour of the composites. Figs. 8-

11 show that the composites generally displayed similar polarization curves and passivity characteristics. Both cathodic and anodic curves have the same aspect due to the same

anodic and cathodic processes occurring of the surface of each of the studied samples.

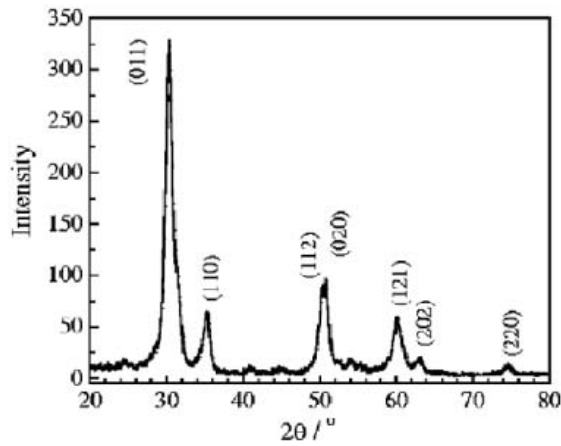
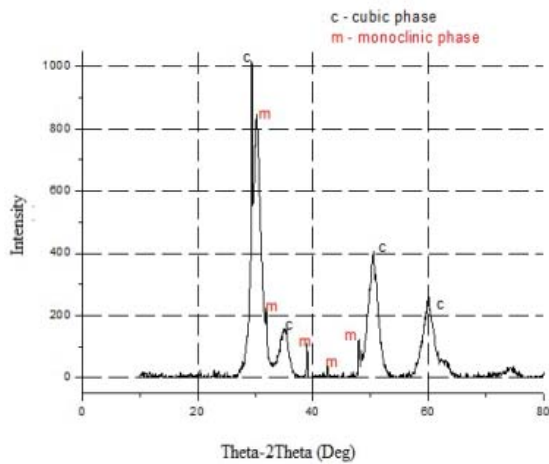


Fig. 4 (a) n-ZrO<sub>2</sub> synthesized at 500 °C; (b) Standard ZrO<sub>2</sub> XRD pattern

In Figs. 8 and 9 which represent 0% ZrO<sub>2</sub> and 2.5% ZrO<sub>2</sub> respectively, we can observe minor change in corrosion potential. Fig. 10 which represents 5% ZrO<sub>2</sub> has a corrosion potential of -1.23 mV which is increased as compared to Fig. 9. Similarly, in Fig. 11, there is clear difference in rate of corrosion, 7.5% ZrO<sub>2</sub> has a corrosion potential of -1.06 mV which is higher than that of base metal (Al-6061) and other samples with lower % of ZrO<sub>2</sub>. The increase in corrosion potential signifies the decrease in corrosion rate. This indicates that the corrosion rate of the Nanocomposite decreases with increase in % of ZrO<sub>2</sub>. The improvement of the corrosion resistance of Al matrix metal due to the addition of ZrO<sub>2</sub> nanoparticles may attribute to the fact that ZrO<sub>2</sub> is being ceramic and remain inert. They are hardly affected by the corrosion medium. Although the corrosion rate of the nanocomposites is lesser than that of the Al matrix metal, the nanocomposites showed also the formation of pits on the surface.

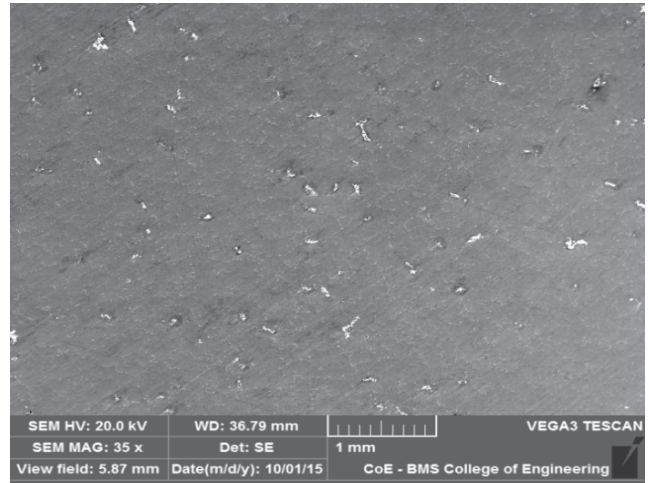


Fig. 6 SEM Micrograph of (7.5% ZrO<sub>2</sub>) Nanocomposite

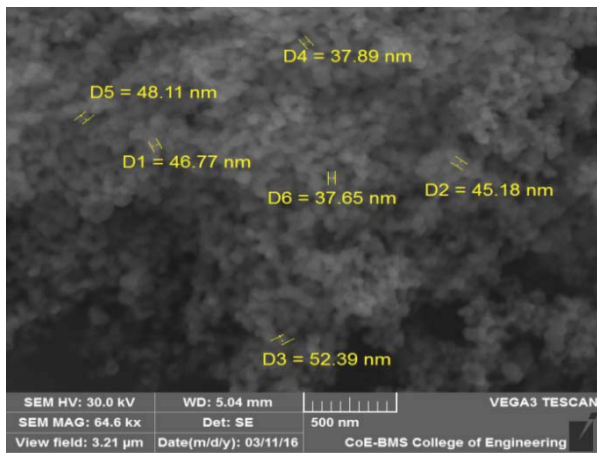


Fig. 5 SEM Micrograph of ZrO<sub>2</sub>

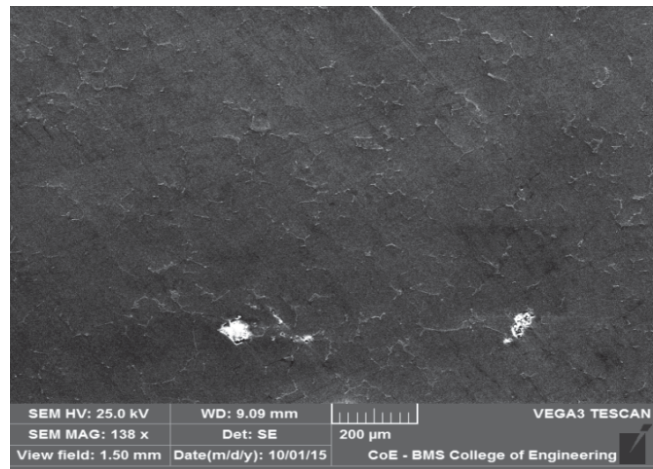


Fig. 7 SEM Micrograph of (7.5% ZrO<sub>2</sub>) Nanocomposite

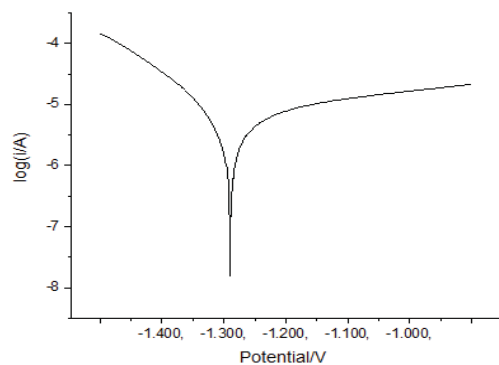


Fig. 8 Tafel plot for corrosion of pure Al

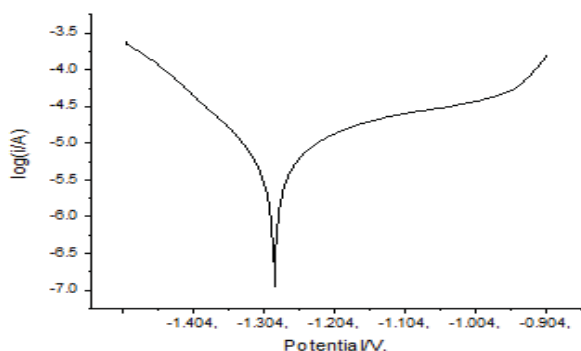


Fig. 9 Tafel plot for corrosion of Al in 2.5% ZrO<sub>2</sub>

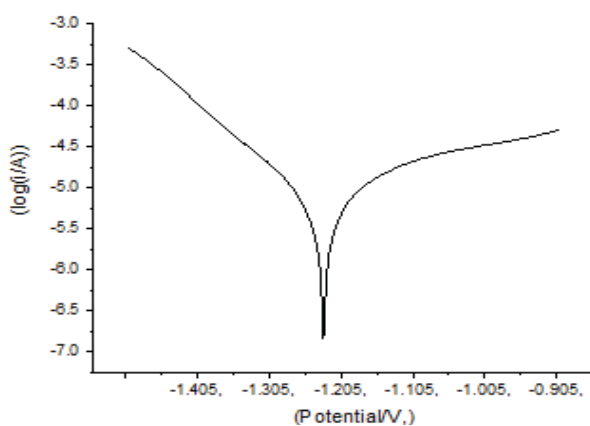


Fig. 10 Tafel plot for corrosion of Al in 5% ZrO<sub>2</sub>

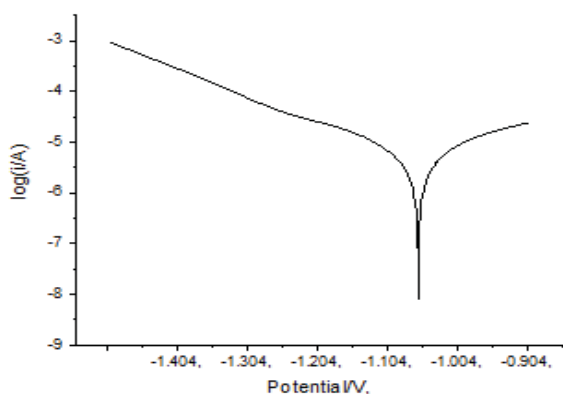


Fig. 11 Tafel plot for corrosion of Al in 7.5% ZrO<sub>2</sub>

TABLE II  
 DIFFERENT CORROSION POTENTIAL FOR DIFFERENT COMPOSITION

S. N	Composition (wt.% of ZrO <sub>2</sub> )	Corrosion potential (mV)
1	0	-1.29
2	2.5	-1.28
3	5	-1.23
4	7.5	-1.06

#### IV. CONCLUSION

Aluminium-ZrO<sub>2</sub> nanocomposites containing 7.5 wt. % of ZrO<sub>2</sub> is synthesized successfully by using stir casting method. The microstructure revealed good interfacial bond between matrix and ZrO<sub>2</sub> particles near uniform distribution of ZrO<sub>2</sub> particles. The corrosion rate of Al-6061 (base metal) is higher than the nanocomposite produced. Also, among the three different weight percentage compositions of ZrO<sub>2</sub> (2.5%, 5%, and 7.5%) in the nanocomposite, the Tafel plot shows the higher rate of corrosion in 2.5 wt.% ZrO<sub>2</sub> when compared to that of 7.5 wt.% ZrO<sub>2</sub>. This shows that on increasing the percentage of ZrO<sub>2</sub> nanoparticles in the nanocomposite, the corrosion rate decreases significantly.

#### ACKNOWLEDGMENT

The authors would like to express their deep sense of gratitude to **TEQIP 1.2.1**, Center of Excellence in Advanced Materials Research, **AICTE** and Management of BMS College of Engineering for support, facilitation and funding the project. Authors also would like to thank Sanjay Ghimire, Roshan Rauniyar, undergraduate students for their involvement in the research work.

#### REFERENCES

- [1] Suma A Rao, Padmalatha, Nayak J. and Shetty A.N., 2006, "Glycyl Glycine as corrosion inhibitor for aluminium silicon carbide composites in hydrochloric acid", Transactions of the SAEST, 41, pp.01-04.
- [2] Aylor D. M., 1987, "Corrosion of Metal Matrix Composites", Metals Hand Book, Ninth Edition, ASM 859.
- [3] Seah K. H. W., Krishna M., Vijayalakshmi V. T. and Uchil J., 2002, "Effects of temperature and reinforcement content on corrosion characteristics of LM 13/ albite composites", Corros. Sci, 44, pp.761-772.
- [4] Terry, B. and Jones, G., 1990, "Metal Matrix Composites: Current Developments and Future Trends in Industrial Research and Applications", Elsevier Advanced Technology/Elsevier Science Publishers Ltd, Amsterdam.
- [5] Govind Nandipati, Dr, Dr. Ravindrakommineni, Dr. Nageswara Rao Damera, Dr. RamanaiahNallu, 2013 "Fabrication and Study of the Mechanical Properties of AA2024 Alloy Reinforced with B4C Nanoparticles using Ultrasonic cavitation method", IOSR Journal of Mechanical and Civil Engineering, Volume 7, Issue 4, PP 01-07.
- [6] Pradheep TirlapurM. MuniprakashMeenu Srivastava "Corrosion and Wear Response of Oxide-Reinforced Nickel Composite Coatings" Journal of Materials Engineering and Performance, July 2016, Volume 25, Issue 7, pp 2563–2569
- [7] V. S. Saji and Joice Thomas, Current Science, Vol. 92, No. 1, 10 JANUARY 2007, pp115.
- [8] B.M. Praveen, T.V. Venkatesha, Y. Arthoba Naik, K. Prashanth "Corrosion studies of carbon nanotubes–Zn composite coating
- [9] Dasappa Ramesh, Ragera Parameshwarappa Swamy, Tumkur Krishnamurthy Chandrashkar 2012, "Corrosion Behaviour of Al6061-Frit Particulate Metal Matrix Composites in Sodium Chloride Solution" Journal of Minerals and Materials Characterization and Engineering, 2013, 1, 15-19. Surface and Coatings Technology · March 2007

- [10] P. D. Reena Kumari, Jagannath Nayak, A. Nityanda Shetty 2011, "Corrosion behaviour of 6061/Al-15 vol. pct. SiC composite and the base alloy in sodium hydroxide solution" *Journal of Arabian chemistry* (2012).
- [11] Muna K. Abbass, Khairia S. Hassan and Abbas S. Alwan, 2015 "Study of Corrosion Resistance of Aluminum Alloy 6061/SiC composites in 3.5% NaCl solution" *International Journal of Materials, Mechanics and Manufacturing*, Vol. 3, No. 1, February 2015.
- [12] S. Skolians (1996), Mechanical Behaviour of Cast SiCp-Reinforced Al-4.5%Cu-1.5% Mg Alloy," *Material Science Engineering* Vol. 210, No.1-2, 1996, pp.76-82.
- [13] C.G. Kang and J.H. Yoon, "The Upsetting Behaviour of Semi-Solid Aluminum Material Fabricated by a mechanical Stirring Process", *Journal of material production Technology*, Vol. 66, No. 1-3,1997, pp.30-38.
- [14] XUY and Chung D.D.L, "Low Volume fabrication particulate performs for making metal-matrix compstion by liquid metal infiltration", *Journal of material science* Vol, 33, No.19 1998 pp.4707-4709
- [15] H. G. Zhu, Y. L. Ai, J. Min, Q. Wu, H. Z. Wang, "Dry sliding wear behaviour of Al-based composites fabricated by exothermic Dispersion reaction in an Al-ZrO<sub>2</sub>-C system".
- [16] J.C. Lee, J. Y. Byun, C.S. Oh, H. K. Seok anh H. I. Lee, "Effect of various processing methods on the Interfacial reaction in SiC/2024 Al Composites," *Acta Materials*, vol.45. No, 12,1998.
- [17] Y. H. Sea and C. G. Kang, "The effect of applied pressure on particle dispersion characteristics and mechanical properties in melt stirring squeeze cast SiC/Al composite," *Journal of materials production technology*, vol-55, No.3-4, 1995, pp 370-379.
- [18] J. S. S Babu, C. G. Kang, H. H. Kim, "Dry sliding behaviour of Aluminum based hybrid composutes with graphite nanofiber-alumina fiber, *Materials & Design* volume 32 issue 7, August 2011, pages 3920-3925.